Adsorption of SO_X and NO_X in activated viscose fibers

ANA CAROLINA O. PLENS, DANIEL L.G. MONARO and APARECIDO R. COUTINHO

Universidade Metodista de Piracicaba, Laboratório de Materiais Carbonosos,
Rodovia SP 306, Km 1, 13451-900 Santa Bárbara d'Oeste, SP, Brasil

ABSTRACT

SO_x and NO_x are emissions resulting from combustion processes and are the main agents that contribute to the formation of acid rain, which causes harm to humans and the environment. Several techniques for removing these pollutants are applied in i.e. oil refineries, thermoelectric that use petroleum oils and vehicular pollution. Among these, highlight the adsorption of contaminants by the usage of activated carbon fibers and activated carbon, which are characterized by high surface area and uniform distribution of pores, providing appropriate conditions for application in processes of removing environmental contaminants. In the present work, activated viscose fibers (AVF) were prepared and applied in adsorption experiments of NO and SO_2. The materials produced showed high values of surface area, with a predominance of micro pores with diameters in the range of 1.0 nm. The AVF had satisfactory performance in the removal of contaminants and are compatible with other synthetic fibers. Thus, the formation of active sites of carbon provides contaminants adsorption, demonstrating that carbon fibers cloth can be applied for the removal of pollutants.

Key words: activated carbon, activated fibers, adsorption, NO_x, SO_x.

INTRODUCTION

Natural, artificial and synthetic fibers are used as raw materials for producing activated carbon fibers, which generally have a high adsorption capacity.

The production process of viscose reached an industrial scale in 1905 through chemical treatment of wood pulp and cotton linter to form the viscose rayon and the acetate (Bastion 2009). The first woven fabric of activated carbon fiber was produced in 1970, using phenolic resin and the viscose rayon as the raw materials from a thermal degradation process of carbonization followed by activation.

In recent decades, woven fabrics of activated carbon fibers (ACF), derived from artificial and synthetic raw materials, were produced with uniform pore distribution and a high surface area. The most important property of ACF is their pore size distribution, with micro pores that provide the capacity to adsorb pollutants from the water and air, when compared with granular activated carbon (Davini 1990, Mochida et al. 2000, Guo et al. 2001, Guo and Lua 2002).

ACFs in the form of felts or woven fabrics have advantages including higher specific surface areas of up to 1,000 $m^2.g^{-1}$, mechanical integrity, easy handling and use in adsorption processes. Furthermore, they have shown potential for being

Correspondence to: Aparecido dos Reis Coutinho
E-mail: arcoutin@unimep.br

used in the removal of various microorganisms, harmful compounds, phenolic, pesticides, dyes, polycyclic aromatic hydrocarbons and volatile organic compounds (VOCs), as well as SO_x and NO_x (Asakura et al. 2004).

The viscose rayon fiber, as the one used in this study, has a retention capacity of 150% of water relative to its dry weight, the ability to withstand temperatures above 190 °C without degradation or color change, of keeping its macroscopically homogeneous body, and a low cost of production (Kuasne 2008).

NO_x Removal by Activated Carbon Fibers

Nitrogen oxides (NO_x, including NO and NO_2) are major pollutants and toxic gases that result in the formation of acid rain, causing the destruction of the ozone layer and therefore posing a threat to humanity and the ecosystem. The removal of NO_x is therefore a global issue that has attracted the attention of many scientists (Wang et al. 2011, Florent et al. 2013).

Among the variety of NO_x gases present in atmospheric air, NO is the most difficult to remove by adsorption because it presents supercritical fluid behavior at room temperature (Verma et al. 2006).

The adsorption technique has advantages in removing gaseous pollutants that include high removal capacity, of implementation in existing processes and its broad array of applications. Furthermore, the adsorption allows further processing of the NO_x accumulated in the pore structure of the adsorbent (Mochida et al. 1985, Rodriguez et al. 1994).

There are other techniques that can be employed to remove NO_x compounds from the air. Firstly, there are preventive actions that entail the optimization of combustion processes to reduce NO_x emissions. The catalytic reduction, effective for treatment and denitrification of flue gases, requires reaction temperatures above 300 °C and the addition of chemical reducing agents such as ammonia and

hydrocarbons, therefore it is not an ecologically viable technique for removing NO_x in the atmosphere at room temperature and from natural agents, as by products formed may affect the biogeochemical cycle (Yao et al. 2010, Sharma et al. 2012).

Other porous materials such as carbon nanofiber materials have become of interest due to their properties, including the high specific surface area and uniform pore size distribution. High specific surface areas produce better contact sites on the surface of reactants, reduce the pore diffusion resistance and enable further processing of the NO_x accumulated in the absorbent structure (Serp et al. 2003, Coelho et al. 2008, Vieira et al. 2009).

Several studies have sought to show the efficiency of systems for the removal of compounds of NO_x. Studies by Guo et al. (2001) showed good results for the catalytic oxidation of NO and NO_2 on activated PAN fibers and activated carbon produced from coconut shells in experiments performed at room temperature. Studies by Mochida et al. (2000) and Shirahama et al. (2002) demonstrated the kinetics and efficiency of the oxidation and reduction of NO in activated carbon fibers. This happens due to the increase of oxygen functional groups on the surface (Mochida et al. 2000).

Porous carbon nanofibers produced from PAN (polyacrylonitrile) fibers via stabilization, carbonization and physical activation in a water vapor atmosphere showed high microporous volume and high surface area. These materials were applied in the removal of NO at room temperature. The proportion of removed NO was higher than 60% for an initial concentration of 20 ppm (Wang et al. 2011).

Teng and Suuberg (1993) studied the reduction of NO with carbon nanofibers produced by the decomposition of methane in the presence of various metallic catalysts between 550-850 K. This material showed a higher reactivity for the reduction of NO than other carbon-based materials such as activated carbon (AC), carbon black, carbon fibers and graphite.

SO$_X$ REMOVAL BY ACTIVATED CARBON FIBERS

SOx are pollutant sulfur oxides mainly consisting of sulfur dioxide (SO$_2$) and a small amount of sulfur trioxide (SO$_3$). SO$_2$ is released in large quantities into the atmosphere, mainly by industries that use fossil fuels, such as oil refineries and automobiles. The atmospheric oxidation caused by this component leads to the formation of acid rain, which results in the abrasion of monuments and buildings, an increase in the acidity of soil and water, and the retardation of the development of flora and aquatic life. SO$_2$ can also react slowly with oxygen to form SO$_3$, which subsequently reacts with water to form sulfuric acid (Harter 1985, Lu and Do 1991, Baird and Cann 2012).

Several methods have been developed to reduce emissions of SO$_2$. Some researchers have proposed rinsing the coal before combustion to remove the sulfur contained in the carbonaceous structure. Others have proposed the application of alkaline chemisorption for desulfurization, resulting in an unregenerated product with low commercial value (Lu and Do 1991, Diez et al. 2014).

Carbon materials have been employed in adsorption techniques for the removal of SO$_2$ due to their high specific surface area and well-defined pore structure, most notably charcoal and activated carbon fibers. The use of these materials has increased because they act as catalysts for the oxidation of SO$_2$ in the presence of O$_2$ and water (Raymundo-Piñero et al. 2000, Diez et al. 2014). Research by Mangun and Debarr (2001) reported the effectiveness of activated carbon fibers for the treatment of ammonia from SOx adsorption.

ACTIVATED CARBON FIBERS

Activated carbon fibers (ACFs) have a high specific surface area, a large number of pores, and excellent flexibility, and can be used in the removal of liquid and gaseous contaminants that pollute the water and air. Their specific properties and physical form allows new applications in adsorption, catalysis and other processes where AC faces limitations in the removal of contaminants (Pastor et al. 1999, Ayranci and Hoda 2005).

In addition to the precursor raw materials, other materials are also used in the carbonization/activation process for preparing activated fibers, such as PAN fibers (Suzuki 1994, Marsh and Rodriguez-Reinoso 2006) and other fibers of natural origin including fiber palm (Foo and Hameed 2011), cotton (Zheng et al. 2014), jute and coconut (Foster et al. 1992, Alves et al. 2010).

The production of ACF is via a thermochemical process involving steps of carbonization and activation at high temperatures, which promotes thermal decomposition of the carbon structure in the presence of oxidizing agents (Smísek and Cerny 1970, Gonzales et al. 1995, Pastor et al. 1999).

Prior to the carbonization, the fibers are heat treated via oxidation (or thermal stabilization) using air at temperatures ranging from 180 to 300 °C under reduced heating rates. This step promotes the modification of the initial fiber structure so that it will withstand high temperatures during the subsequent carbonization and activation processes.

During the step of thermal stabilization, the amount of oxygen present in the structure ranges from 8 - 12%. In cases where the presence of oxygen is less than 8%, the stabilization results in a low amount of carbon (approximately 12%), leading to fiber deterioration. The stabilization of viscose in an air atmosphere increases the yield during the carbonization step to the range of 18 to 24% (Smísek and Cerny 1970, Gonzales et al. 1995, Pastor et al. 1999).

After the step of stabilization, the fibers are subjected to a carbonization process in an inert atmosphere at temperatures between 400 - 1,100 °C, which increases the carbon content to more than 90%. Heating rates below 3 °C.min^{-1} result in an increased yield of carbonaceous material, producing fibers with a poorly developed amorphous porous structure.

The physical activation step occurs at temperatures ranging from 800 to 1,100 °C in the presence of an oxidizing atmosphere. Initially, the amorphous carbon reacts with the oxidizing agent, clearing and forming new pores. This amendment promotes the increase of micro pores that act as active sites and are responsible for the high adsorption capacity.

Temperature is a major factor in the activation step, as the presence of carbon dioxide at temperatures of 800 °C or higher results in materials with a high adsorption capacity due to the higher micro pore volume (V_{micro}), and also due reduction in the volume of mesopores (V_{meso}).

The objective of this research is to prepare activated viscose fibers (AVF) to assess their potential for use in adsorption to remove pollutants NO_x and SO_x through increasing the specific surface area and uniformity in relation to the distribution of the pores. The adsorption capacity was analyzed in relation to the pore volume and the saturation time of AVF.

MATERIALS AND METHODS

PREPARATION OF ACTIVATED VISCOSE FIBERS

Viscose rayon fabrics were provided by S.A. Fabril Scavone located in the city of Itatiba, state of São Paulo, Brazil, with a thickness of 3 mm, width of 1 m, length of 10 m and an area density of 727.96 g.m^{-2}. The samples were composed of 100% viscose rayon with 16-24% elongation and thermal degradation between 180 °C and 205 °C. The specifications were provide by the manufacturer.

Activated viscose fibers (AVF) were produced by means of a static process in which the feedstock was subjected to a single stage of carbonization and activation. The fabric were cut into strips 530 mm long and 70 mm wide and arranged in a spiral inside the furnace.

The experimental system was composed of a tubular electric furnace mounted vertically, and a quartz reactor of 800-mm in length and 56-mm in diameter, which was coupled to a control system to allow gas flow of CO_2 and N_2. The experimental setup was performed at a constant heating rate of $\alpha_1 = 2.5$ °C.min^{-1}. Samples were heated from room temperature (T_1) to 250 °C (T_2) in an inert atmosphere with a flow rate of 300 ml.min^{-1}, followed by a single isothermal stage of 2h ($t_1 \rightarrow t_2$), with a subsequent rise in temperature up to 800 °C (T_3) in an inert atmosphere combined with a flow rate of CO_2 of 100 ml.min^{-1}. The experiments were then repeated with $\alpha_2 = 5$ °C min^{-1} and $\alpha_3 = 10$ °C min^{-1}, keeping the other conditions the same, as shown in Figure 1.

POROUS STRUCTURE OF THE SAMPLES

The experiments to characterize the porous structure of the AVF were performed by the BET technique to produce adsorption/desorption isotherms in N_2 at 77K, using Autosorb-1MP equipment from Quantachrome. The analysis for determining the true density of the samples was performed by helium pycnometry using an Ultrapycnometer 1,000 from Quantachrome.

SO_x AND NO_x ADSORPTION

The adsorption experiments were conducted with 99.0% purity SO_2 and NO gases, provided by White Martins Praxair Inc. Company, dissolved in 2,000 ppm N_2 as a carrier gas to obtain concentrations of 250 and 100 ppm, respectively. Analyses were performed using a Lancon III Land Instruments International gas analyzer, as shown in Figure 2.

RESULTS AND DISCUSSION

The samples of AVF had a yield of 20.4±1.1%, similar to that of activated PAN fibers (Zaini et al. 2010) and activated carbons produced from biomass (Tan et al. 2008, Asadullah et al. 2010). They also showed a contraction of 33.3±1.1% in length and a true density of 1.46 g.cm^{-3}.
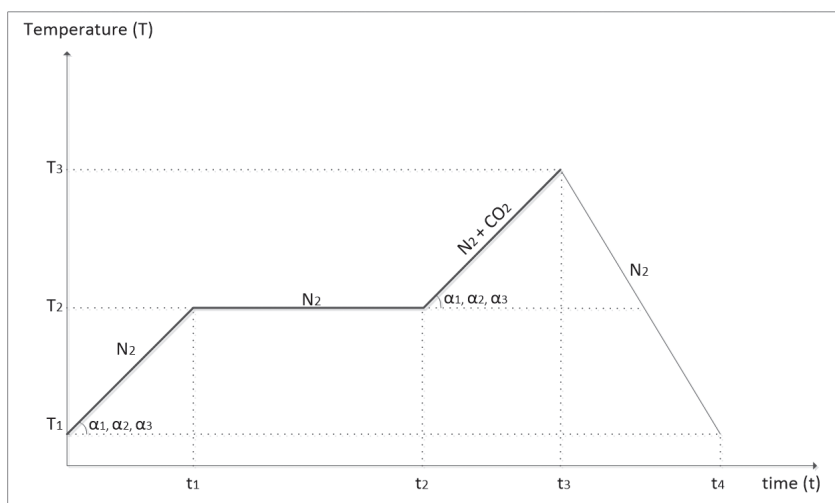
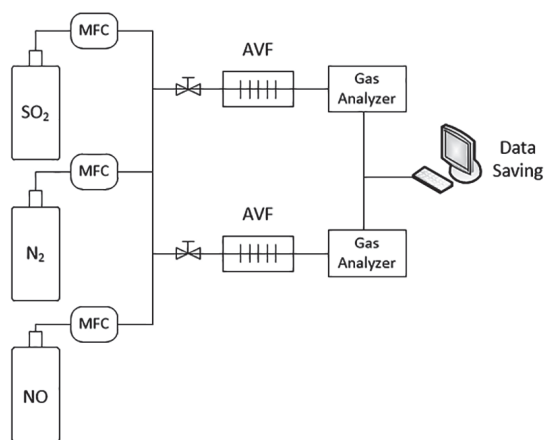**Figure 1 -** Diagram of thermal degradation during AVF preparation.

Figure 2 - Experimental system for removal of SO$_2$ and NO gases by AVFs.
(MFC: Mass flow control. AVF: activated viscose fibers).

POROUS STRUCTURE OF THE SAMPLES - ISOTHERMS OF ADSORPTION/DESORPTION

Experiments were conducted on AVF samples to obtain adsorption and desorption isotherms of N$_2$, and results were similar among samples. Thus, only one sample was chosen to represent the isotherms obtained, as shown in Figure 3.

The curve shows the typical behavior of type I isotherm, characterized by the existence of a plateau that begins at a relatively low pressure which is characteristics of the adsorption mechanism of the micro pores. A hysteresis phenomenon was also observed, which is associated with condensation and evaporation of the liquid inside the pores resulting in different saturation vapor pressures, which is due to the geometry of the pores.

Tables I, II and III show the results obtained from the adsorption/desorption isotherms of the AVF sample under N$_2$ flow at 77K. It is noteworthy that the difference observed was due to the different heating rates used for activation process.

Results show that the AVF samples have a high fraction of micro pores (%).

There is a variation of approximately 10% in the SSA (specific surface area) for samples prepared using a heating rate of 10 °C.min^{-1} when compared to samples prepared using a heating rate of 2.5 °C. min^{-1}. This percentage change was also observed for other parameters, most notably the micro pore volume (V$_{micro}$), which is responsible for defining the specific surface area value.

The SSA and micro pore fractions exhibited higher values than those prepared by Gaur et al. (2006) that used the same raw materials (viscose rayon and PAN), temperature and oxidation atmosphere. However, AVF showed lower values than PAN fibers prepared under the same oxidation atmosphere but with a higher activation temperature, tested by Marcuzzo et al. (2014).
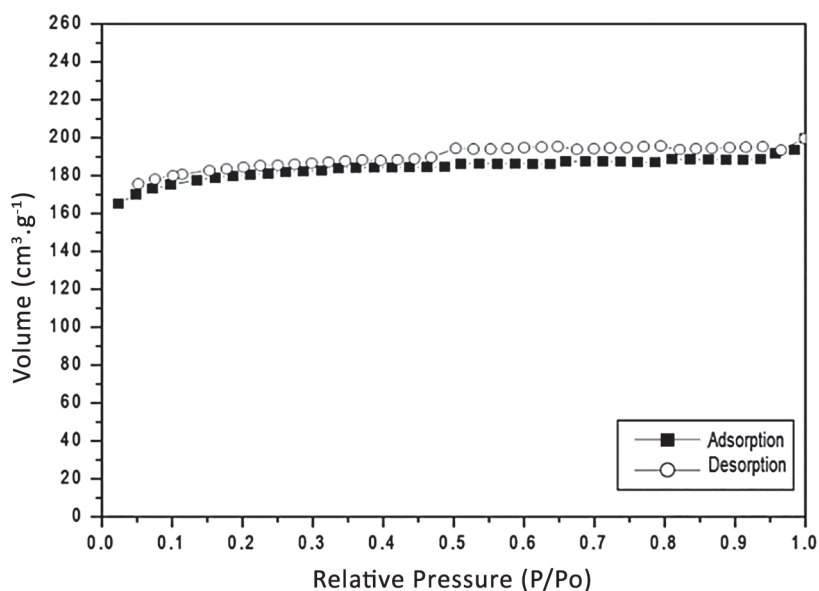
Figure 3 - Isotherm of AVF sample under N_2 flow at 77K.

TABLE I

**Parameters of the porous structure of AVFs
activated under a heating rate of 2.5 °C.min⁻¹.**

Sample	V_p $(cm^3.g^{-1})$	$d_{average}$ (nm)	V_{micro} $(cm^3.g^{-1})$	A_{micro} $(m^2.g^{-1})$	ASE $(m^2.g^{-1})$	Fraction of micro pores (%)
AVF1	0.310	2.386	0.280	509.1	519.0	90.3
AVF2	0.312	2.385	0.279	505.6	514.5	89.4
AVF3	0.317	2.385	0.277	504.1	513.2	87.4
Average ± δ	0.313 ± 0.003	2.385 ± 0.001	0.279 ± 0.001	505.3 ± 2.7	515.6 ± 2.5	89.3 ± 1.21

TABLE II

**Parameters of the porous structure of AVFs
activated under a heating rate of 5 °C.min⁻¹.**

Sample	V_p $(cm^3.g^{-1})$	$d_{average}$ (nm)	V_{micro} $(cm^3.g^{-1})$	A_{micro} $(m^2.g^{-1})$	SSA $(m^2.g^{-1})$	Fraction of micro pores(%)
AVF4	0.322	2.390	0.291	525.2	542.1	90.4
AVF5	0.336	2.391	0.293	528.0	544.4	87.2
AVF6	0.339	2.391	0.295	531.1	547.2	87.0
Average ± δ	0.332 ± 0.009	2.391 ± 0.001	0.293 ± 0.002	528.1 ± 2.9	544.7 ± 2.6	88.2 ± 1.9

TABLE III

**Parameters of the porous structure of AVFs
activated under a heating rate of 10 °C.min⁻¹.**

Sample	V_p $(cm^3.g^{-1})$	$d_{average}$ (nm)	V_{micro} $(cm^3.g^{-1})$	A_{micro} $(m^2.g^{-1})$	ASE $(m^2.g^{-1})$	Fraction of micro pores(%)
AVF7	0.344	2.389	0.312	550.5	572.2	90.7
AVF8	0.345	2.390	0.315	553.3	575.6	91.3
AVF9	0.349	2.392	0.319	558.0	578.4	91.4
Average ± δ	0.346 ± 0.003	2.390 ± 0.002	0.315 ± 0.004	553.9 ± 3.8	575.5 ± 3.1	91.1 ± 0.4

Using the NLDFT/Monte Carlo method, which does not require consideration of the geometry of the pore and can be applied to the entire range of meso and micro-porosity, it is possible to obtain the distribution of the pores of the sample of AVF, as shown in Figure 4.
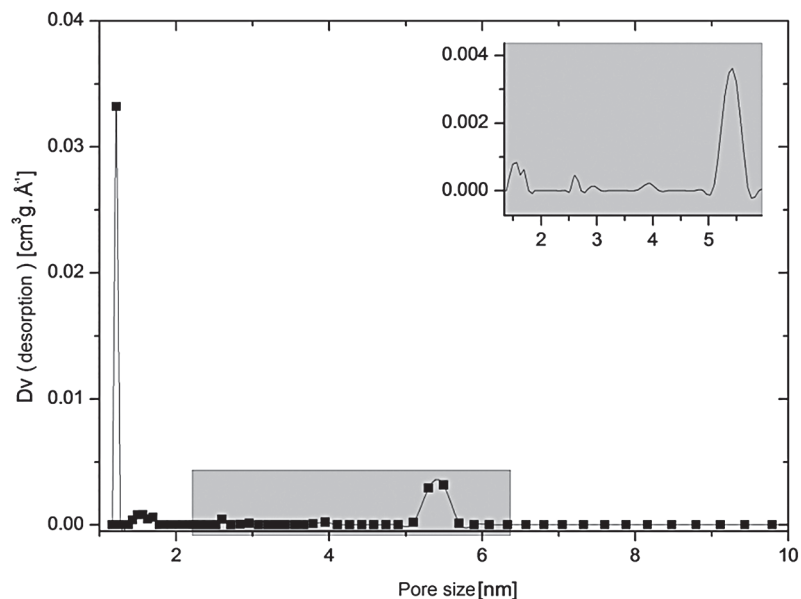
Figure 4 - Pore distribution of AVF sample based on adsorption/desorption isotherm using NLDFT/Monte Carlo method.

The curve of the pore diameter distribution has prominent peaks in the regions of 1.0 nm, corresponding to the micro pore region, and 5.4 nm, corresponding to the transition between the mesopore and macropore regions.

The analysis of the porous structure of AVF shows that the material structure has a micro pore fraction of approximately 90%, which is fundamental as it favors the adsorption of contaminants.

SO$_2$ ADSORPTION

Figure 5 shows the time evolution of saturation of the sample of the original viscose fibers (OVF) exposed to the SO$_2$ gas stream. The adsorption front experiences an abrupt increase of the amount of adsorbed SO$_2$ after approximately 1 min and reaches saturation after approximately 8 min.

This behavior is explained by the absence of active sites due to the negligible pore volume, resulting in an inefficient adsorption of SO$_2$.

Samples of AVF were subjected to the same process of SO$_2$ adsorption and showed superior performance in relation to OVF.

Samples AVF 1 and AVF 2 were produced under the same conditions and showed similar SO$_2$ adsorption with the adsorption fronts at approximately 100 and 120 min, respectively (Fig. 6). For both samples, the curves experienced a sharp rise at approximately 250 min and then reached a saturation level.

Figure 7 shows the evolution of SO$_2$ adsorption in samples AVF 6 and AVF 9. It can be observed that both samples showed an adsorption front of around 220 min, followed by a sharp rise at approximately 300 min before subsequently reaching complete saturation.

The adsorption values of samples AVF 6 and AVF 9 were higher than those of samples AVF 1 and AVF 2 due to their larger pore volume and surface area. Thus, an increase in the SO$_2$ adsorption front presented in
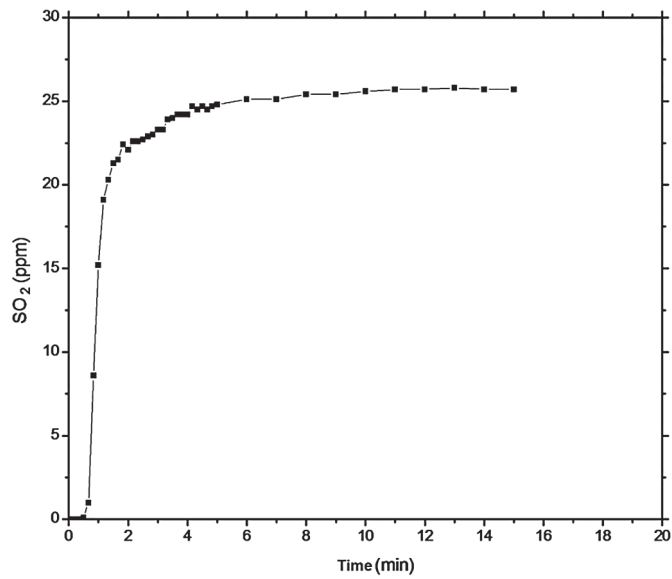
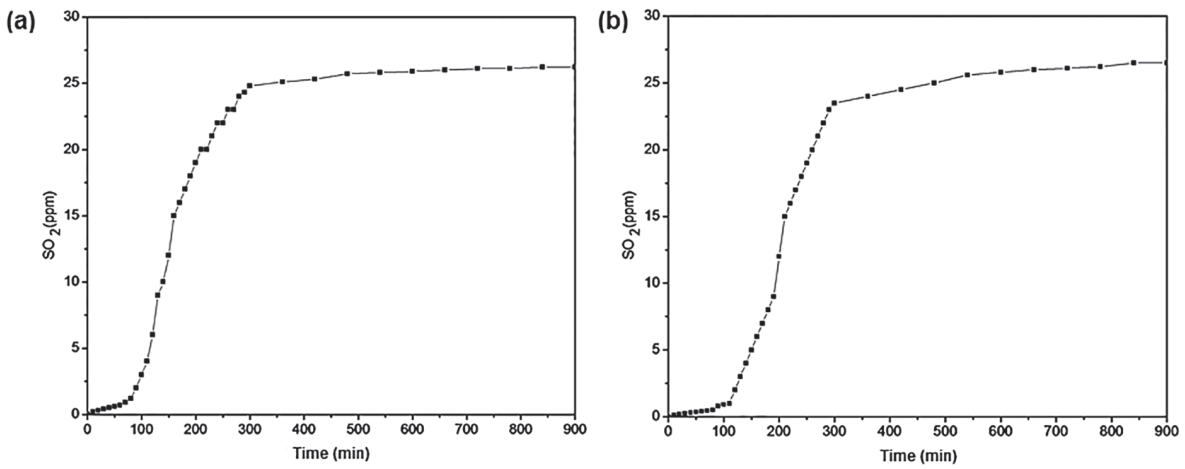**Figure 5 -** Evolution of SO$_2$ adsorption for the original viscose fiber.

Figure 6 - Evolution of SO$_2$ adsorption of samples **(a)** AVF 1 and **(b)** AVF 2.
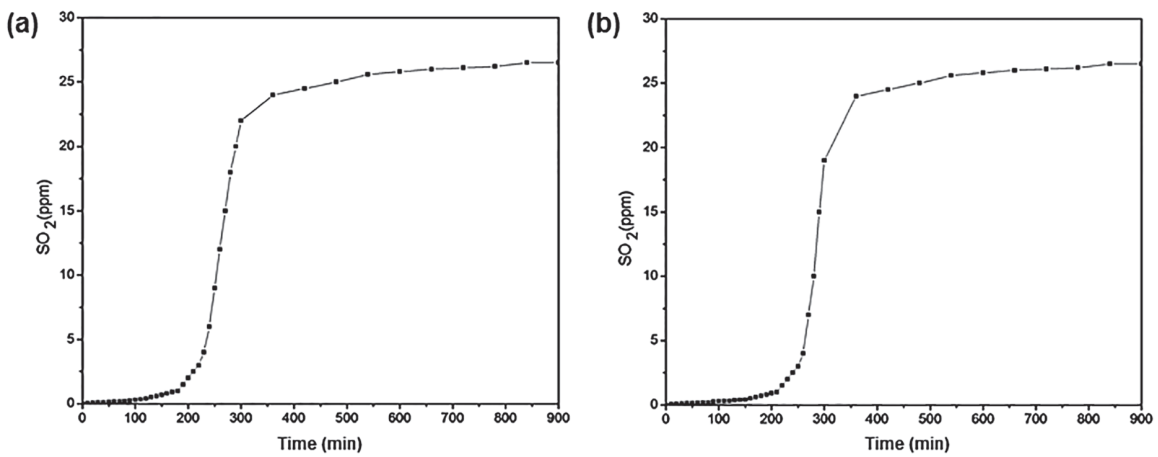

Figure 7 - Evolution of SO$_2$ adsorption of samples **(a)** AVF 6 and **(b)** AVF 9.

AVF was due to an increase in the pore volume and the specific surface area, which introduces new active sites for the promotion of adsorption.

AVF in this study presented lower values for the adsorption of SO$_2$ and the saturation time than those obtained by Mochida et al. (2000). However, the samples exhibited higher values of saturation than the results obtained by Gaur et al. (2006).

NO ADSORPTION

Figure 8 shows the time evolution of the saturation of the original sample of viscose fibers (OVF) exposed to a NO gas flow. It can be observed that the sample has an OVF adsorption front of less than 1 min, followed by an abrupt increase in the amount of NO adsorbed, reaching saturation below 25 ppm for about 5 min and remaining constant for larger time intervals. It is noteworthy that a similar behavior was also observed for untreated samples during the SO$_2$ adsorption trial. This indicates that the original non-activated samples do not have active sites that enable extensive physisorption and chemisorption of SO$_x$ and NO$_x$.

For comparison purposes, samples were processed under the same activation conditions for the adsorption of SO$_2$ and NO to assess the performance of the process in removing different contaminants.

Samples AVF 1 and AVF 2 were produced under the same conditions and showed similar NO adsorption behavior (Fig. 9). There was an initial front at approximately 50 min, followed by a sharp increase between 50 - 100 min and a saturation plateau at approximately 200 min.

Figure 10 shows the evolution of NO adsorption by samples AVF 6 and AVF 9. It may be observed that the adsorption fronts occurred at 70 and 120 min, respectively. In both samples, a sharp increase occurred around 300 min after reaching a level of complete saturation.

It may be observed that the values of the adsorption front in samples AVF 6 and AVF 9 were superior to those of samples AVF 1 and AVF 2. The increasing values across the adsorption of NO observed in AVFs were due to the increased pore volume.
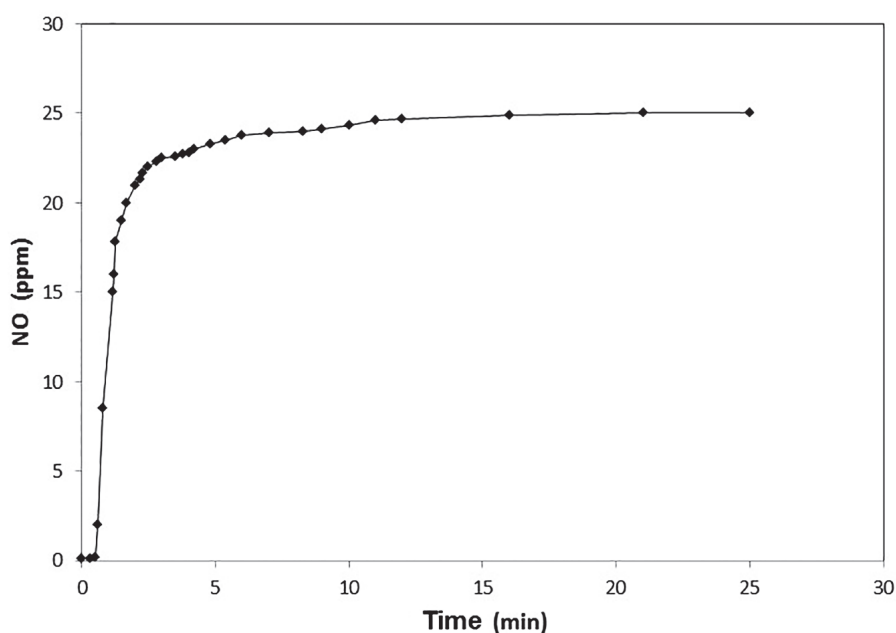

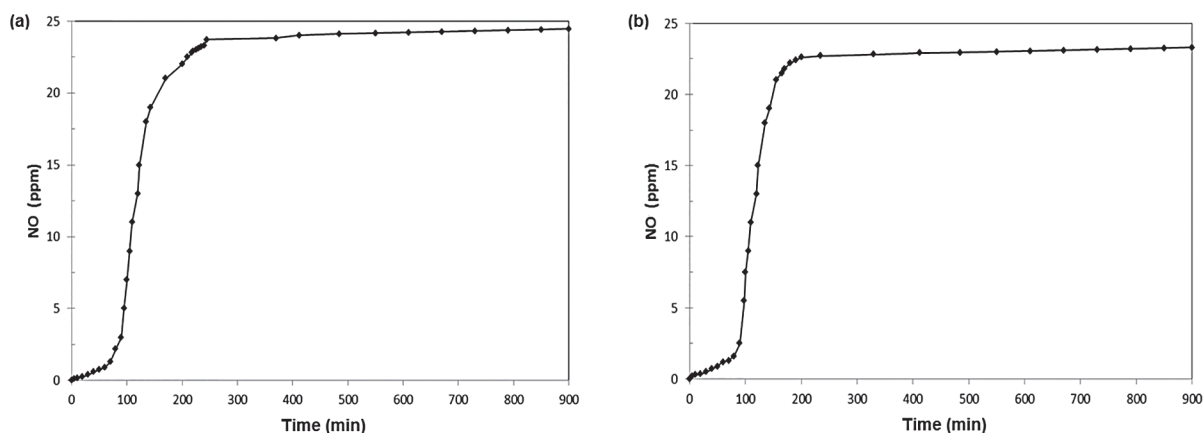**Figure 8 -** Evolution of NO adsorption for the original viscose fiber.

Figure 9 - Evolution of NO adsorption of samples **(a)** AVF 1 and **(b)** AVF 2.
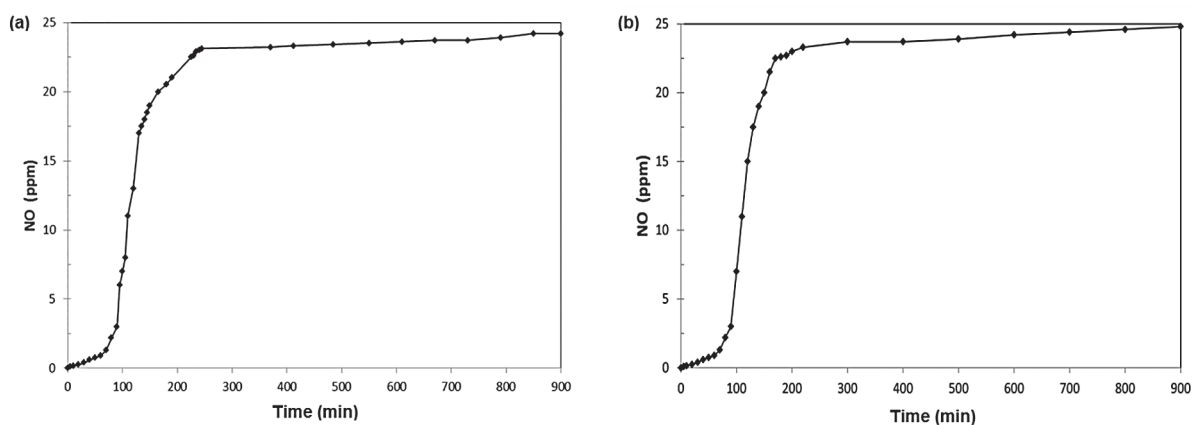

Figure 10 - Evolution of NO adsorption of samples **(a)** AVF 6 and **(b)** AVF 9.

CONCLUSIONS

The activated viscose carbon fiber samples (AVF) showed high surface area values and a microporous structure having a micro pore fraction of approximately 90% and an average pore diameter of 1.0 nm.

Experiments for SO_2 and NO adsorption were used to observe the effectiveness of AVF as an adsorbent in the removal of contaminants. The formation of active sites of carbon develops an initial region called the adsorption front that is responsible for the physisorption and chemisorption phenomena in pollutant removal. The complete pore saturation observed is compatible with the experiments performed with activated carbon fibers produced from PAN fibers.

RESUMO

As emissões de SO_x e NO_x resultam dos processos de combustão e são os principais agentes contribuintes para a formação da chuva ácida, que causa danos aos seres humanos e ao ambiente. Várias técnicas para remoção desses poluentes são aplicadas, por exemplo, nas refinarias de petróleo, termoelétricas que utilizam óleos derivados de petróleo e poluição veicular. Dentre eles, destaca-se a adsorção de contaminantes pela utilização de fibras de carbono ativadas e carvões ativados, os quais se caracterizam pela elevada área superficial e distribuição uniforme de poros, proporcionando condições adequadas para a aplicação nos processos de remoção dos contaminantes ambientais. No presente trabalho, fibras de viscose ativadas (FVA) foram preparadas e aplicadas em experimentos de adsorção de NO e SO_2. Os materiais

produzidos apresentaram altos valores de área superficial, com predominância de microporos com diâmetros na faixa de 1,0 nm. As FVA apresentaram desempenho satisfatório na remoção dos contaminantes e são compatíveis com outras fibras sintéticas. Assim, a formação de novos sítios ativos de carbono proporciona a adsorção dos contaminantes, demonstrando que os tecidos de fibras de carbono podem ser aplicados na remoção de poluentes.

Palavras-chave: carvão ativado, fibra ativada, adsorção, NOx, SOx.

REFERENCES

ALVES C, FERRÃO PMC, SILVA AJ, REIS LG, FREITAS M, RODRIGUES LB AND ALVES DE. 2010. Ecodesign of automotive components making use of natural jute fiber composites. J Clean Prod 18: 313-327.

ASADULLAH M, ASADUZZAMAN M, KABIR MS, MOSTOFA MG AND MIYAZAWA T. 2010. Chemical and structural evaluation of activated carbon prepared from jute sticks for Brilliant Green dye removal from aqueous solution. J Hazard Mat 174: 437-443.

ASAKURA R, MORITA M, MARUYAMA K, HATORI H AND YAMADA Y. 2004. Preparation of fibrous activated carbons from wood fiber. J Mater Sci 39: 201-206.

AYRANCI E AND HODA N. 2005. Adsorption kinetics and isotherms of pesticides on activated carbon-cloth. Chem 60: 1600-1607.

BAIRD C AND CANN M. 2012. Environmental Chemistry, n. 5, W.H. Freeman and Company, New York, p. 20-22.

BASTION EYO. 2009. Guia técnico ambiental da indústria têxtil. CETESB. São Paulo.

COELHO NMD, FURTADO JLB, PHAM-HU C AND VIEIRA R. 2008. Carbon nanofibers: a versatile catalytic support. Mat Res 11: 353-357.

DAVINI P. 1990. Adsorption and desorption of SO$_2$ on active carbon: The effect of surface basic groups. Carbon 28: 565-571.

DIEZ N, ALVAREZ P, GRANDA M, BLANCO C, GRYGLEWICZ G, WRÓBEL-IWANIEC I, SLIWAK A, MACHNIKOWSKI J AND MENENDEZ R. 2014. Tailoring micro-mesoporosity in activated carbon fibers to enhance SO$_2$ catalytic oxidation. J Colloid Interface Sci 428: 36-40.

FLORENT M, TOCCI M AND BANDOSZ TJ. 2013. NO$_2$ adsorption at ambient temperature on urea-modified ordered mesoporous carbon. Carbon 63: 283-293.

FOO KY AND HAMEED BH. 2011. Microwave-assisted preparation of oil palm fiber activated carbon for methylene blue adsorption. Chem Eng J 166: 792-795.

FOSTER KL, FUERMAN RG, ECONOMY J, LARSON SM AND ROOD MJ. 1992. Adsorption characteristics of trace volatile organic compounds in gas streams onto activated carbon fibers. Chem Mat 4: 1068-1073.

GAUR V, SHARMA A AND VERMA N. 2006. Preparation and characterization of ACF for the adsorption of BTX and SO$_2$. Chem Eng and Process 45: 1-13.

GONZALES MT, SEPULVEDA-ESCRIBANO A AND RODRIGUEZ-REINOSO F. 1995. Correlation between surface areas and micropore volumes of activated carbons obtained from physical adsorption and immersion calorimetry. Langmuir 11: 2151-2155.

GUO J AND LUA AC. 2002. Microporous activated carbons prepared from palmshell by thermal activation and their application to sulfurdioxide adsorption. J Colloid Interface Sci 251: 242-247.

GUO ZC, XIE YS, HONG IY AND KIM JY. 2001. Catalytic oxidation of NO to NO$_2$ on activated carbon. Energy Convers Manage 42: 2005-2018.

HARTER P. 1985. Sulphates in the Atmosphere, IEA Coal Research, n. 14-15, Lower Grosvenor Place, London, p.155.

KUASNE A. 2008. Fibras Têxteis. Santa Catarina: CEFET/SC.

LU GQ AND DO DD. 1991. Preparation of economical sorbents for SO2 and NOx removal using coal washery reject. Carbon 29: 207-213.

MANGUN CL AND DEBARR JA. 2001. Economy, J. Adsorption of sulfur dioxide on ammonia-treated activated carbon fibers. Carbon 39: 1689-1696.

MARCUZZO JS, CUÑA A, TANCREDI N, POLIDORO HA, OTANI S AND OTANI C. 2014. Microporous activated carbono fiber felt produced from brasilian textile pan fiber. X Encontro Brasileiro sobre Adsorção. Guarujá, SP, Brasil.

MARSH H AND RODRIGUEZ-REINOSO F. 2006. Activated Carbon. N. 1, Elsevier, Amsterdam.

MOCHIDA I, KORAI Y, SHIRAHAMA M, KAWAMO S, HADA T, SEO Y, YOSHIKAWA M AND YASUTAKE A. 2000. Removal of SO$_x$ and NO$_x$ over activated carbon fibers. Carbon 38: 227-239.

MOCHIDA I, OGAKI M, FUJITSU H, KOMATSUBARA Y AND IDA S. 1985. Reduction of NO by activated PAN-carbon fiber. Fuel 64: 1054-1057.

MOCHIDA I, SHIRAHAMA N, KAWANO S, KORAI Y, YASUTAKE A, TANOURA M, FUJI S AND YOSHIKAWA Y. 2000. NO oxidation over activated carbon fiber (ACF). Part 1. Extended kinetics over a pitch based ACF of very large surface area. Fuel 79: 1713-1723.

PASTOR AC, RODRÍGUEZ-REINOSO F, MARSH H AND MARTINEZ MA. 1999. Preparation of activated carbon cloths from viscous rayon. Part I. Carbonization procedures. Carbon 37: 1275-1283.

RAYMUNDO-PIÑERO E, CAZORLA-AMOROS D, SALINAS-MARTINEZ C AND LINARES-SOLANO A. 2000. Factors controlling the SO$_2$ removal by porous carbons: relevance of the SO oxidation step. Carbon 38: 335-344.

RODRIGUEZ NM, KIM MS AND BAKER RTK. 1994. Carbon nanofibers - a unique catalyst support medium. J Phys Chem 98: 13108-13111.

SERP P, CORRIAS M AND KALCK P. 2003. Carbon nanotubes and nanofibers in catalysis. Appl Catal A 253: 337-358.

SHARMA M, VYAS R AND SINGH K. 2012. A review on reactive adsorption for potential environmental applications. Adsorpt 1: 1-28.

SHIRAHAMA N, MOON SH, CHOI KH, ENJOJI T, KAWANO S, KORAI Y, TANOURA M AND MOCHIDA I. 2002. Mechanistic study on adsorption and reduction of NO_2 over activated carbon fibers. Carbon 40: 2605-2611.

SMÍSEK M AND CERNY S. 1970. Active carbon: manufacture, properties and applications. Elsevier Publishing Comp., n. 1, Amsterdam-London-New York, p. 56-78.

SUZUKI M. 1994. Activated carbon fiber: fundamentals and applications. Carbon 32: 577-586.

TAN IAW, AHMAD AL AND HAMEED BH. 2008. Optimization of preparation conditions for activated carbons from coconut husk using response surface methodology. Chem Eng J 137: 462-470.

TENG HS AND SUUBERG EM. 1993. Chemisorption of nitric oxide on char - reversible nitric oxide sorption. J Phys Chem 97: 478-483.

VERMA N, ADAPA S AND GAUR V. 2006. Catalytic oxidation of NO by activated carbon fiber (ACF). Chem Eng J 116: 25-37.

VIEIRA R, LOUIS B AND PHAM-HUU C. 2009. Carbon nanofibers: a versatile catalyst support. L'Actual Chim 1: 14-18.

WANG M, HUANG ZH, SHIMOHARA T, FEIYUKANG F AND LIANG K. 2011. NOx removal by electrospun porous carbon nanofibers at room temperature. Chem Eng J 170: 505-511.

YAO GH, GUI KT AND WANG F. 2010. Low-temperature De-NOx by selective catalytic reduction based on iron-based catalysts. Chem Eng Technol 33: 1093-1098.

ZAINI MAA, AMANO Y AND MACHIDA M. 2010. Adsorption of heavy metals onto activated carbons derived from polyacrylonitrile fiber. J Hazard Mat 180: 552-560.

ZHENG J, ZHAO Q AND YE Z. 2014. Preparation and characterization of activated carbon fiber (ACF) from cotton woven waste. Appl Surf Sci 299: 86-91.